Coverage dependence of the Landau Fermi-liquid parameters F_0^A and F_1^S for ^{3}He on thin ^{4}He films

H. Akimoto,* J. D. Cummings, and R. B. Hallock
Laboratory of Low Temperature Physics, Department of Physics, University of Massachusetts, Amherst, Massachusetts 01003, USA
(Received 21 September 2005; published 12 January 2006)

We present the results from our heat capacity experiments on two-dimensional liquid ^{3}He on thin superfluid ^{4}He films adsorbed to Nuclepore. Measurement of the specific heat at low temperatures ($40 < T < 220$ mK) over a ^{3}He coverage range 0.02–0.93 atomic layers on 3.14 and 4.33 bulk-density atomic layer ^{4}He films enables the determination of the ^{3}He quasiparticle effective mass m^*. Combining these results with previous ^{3}He NMR magnetic susceptibility measurements for the same substrate and ^{4}He coverages permits the determination of the two-dimensional Landau Fermi-liquid parameters F_0^A and F_1^S.

DOI: 10.1103/PhysRevB.73.012507 PACS number(s): 67.60.Fp, 67.70.+n

A bulk ^{3}He-^{4}He mixture can phase separate into a ^{3}He-rich phase and a ^{3}He-poor phase, with the ^{3}He-rich phase floating on top of the ^{3}He-poor phase.[1] When the temperature is low enough and the ^{3}He concentration is extremely low, instead of this phase separation the ^{3}He atoms occupy a bound state[2] on the free surface of essentially pure ^{4}He. The bound ^{3}He atoms on the bulk superfluid ^{4}He behave as a two-dimensional (2D) Fermi gas. Interaction effects dress the bare ^{3}He mass, m_3, and it is customary to refer to the interacting ^{3}He atom as a quasiparticle with an effective mass[3] $m^* > m_3$.

For the case of small amounts of ^{3}He on a thin ^{4}He film, the ^{3}He will occupy a surface state similar to that of the bulk case.[4–6] However, the close proximity of the underlying substrate modifies the potential felt by the ^{3}He and creates a discrete set of 2D states with the excited states believed to be located in[7] the film.[8,9] The promotion from the surface state to the first excited state has been experimentally observed[10,11] and can be explained in terms of a set of Fermi disks, analogous to the three-dimensional Fermi sphere. These disks are a result of the proximity of the surface which creates an energy spectrum that is continuous in two degrees of freedom, but discrete in the third (i.e., perpendicular to the substrate). Thus, the more typical three-dimensional Fermi sphere is reduced to a set of Fermi disks. Once the ^{3}He coverage is such that the first Fermi disk is full, a second disk appears and the ^{3}He occupies the second Fermi disk consistent with the requirements of the Pauli exclusion principle.[4] For the presentation here, the ^{3}He will be at relatively low coverage and typically only a single disk will be occupied.

The Fermi temperature, T_F, is proportional to the areal density of fermions N/A, where A is the area covered by the fermions, and for a 2D system of N_3 ^{3}He atoms

$$T_F = \frac{h^2 N_3}{4\pi k_B m^* A}, \tag{1}$$

where m^* is the effective mass of the ^{3}He quasiparticle. In the experiments that we report here A is fixed, but T_F can be changed by adjusting the number of ^{3}He atoms. This allows data to be taken with different values of T_F. Landau's Fermi-liquid theory is used to explain the interactions among these quasiparticles. The theory starts with the free Fermi gas model and uses a perturbation method to introduce the interactions among the atoms.[12] The effective mass can be described in terms of the hydrodynamic mass m_H which arises due to the ^{3}He-^{4}He interactions at the free surface of the ^{4}He film, and F_1^S, the Fermi parameter that characterizes ^{3}He p-wave interactions:

$$m^* = m_H(1 + F_1^s/2). \tag{2}$$

When considering the heat capacity of a 2D Fermi system, there are two temperature regimes that are relevant. One, the degenerate regime, occurs for temperatures much less than the Fermi temperature $T \ll T_F$. For this case, the heat capacity is given by

$$C = \frac{\pi k_B^2 m^* A T}{3\hbar^2}. \tag{3}$$

We note here that for the degenerate case the heat capacity is linear in temperature but is independent of the number of ^{3}He atoms. The other case is the Boltzmann, or classical, regime and this occurs for $T \gg T_F$. Fermi statistics do not play a factor at these higher temperatures and the heat capacity is given by

$$C = N_3 k_B. \tag{4}$$

In the classical case, as opposed the the degenerate one, the heat capacity is proportional to the number of ^{3}He atoms and independent of temperature.

In this work, we present measurements from our heat capacity experiments on ^{3}He-^{4}He mixture films.[13–17] These results allow a determination of the effective mass m^* as a function of ^{3}He coverage. In the work we report here we extend our previous results[14] to lower temperatures and report results for a second ^{4}He film thickness. Combination of these results with the data of Higley *et al.*[11] allows the determination and comparison of the first two Fermi liquid parameters F_0^A and F_1^S for the ^{3}He in the first Fermi disk as a function of ^{3}He coverage for two different ^{4}He film thickness values.

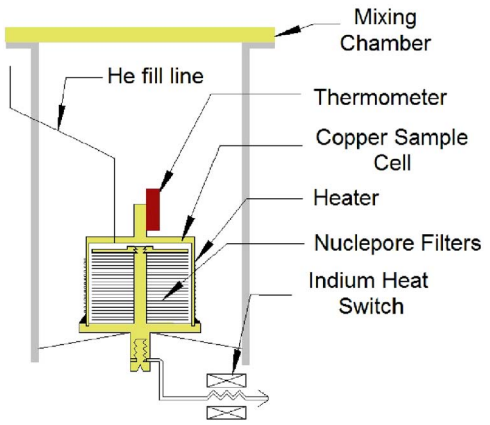

FIG. 1. (Color online) A schematic diagram of the calorimeter used in this work.

The calorimeter used for our measurements is shown schematically in Fig. 1. It consists of a high conductivity copper cell that is filled with 1416 Nuclepore[18] filter disks giving a effective surface area of 23.96 m^2. Each 10 μm disk, with pores of diameter 200 nm at a density of 3×10^8 pores/cm^2, is center punched and gently pressed onto a central copper post to increase the thermal contact.[14] Nuclepore is used as the substrate because of its large surface area and its ability to support films of up to several atomic layers without capillary condensation.[19] To apply heat to the calorimeter, an electric current is applied to a Pt-W wire heater that is wound in a non-magnetic fashion around the cell. The sample cell is connected to the mixing chamber of a dilution refrigerator via an indium heat switch,[20] which allows either thermal contact with, or isolation from, the mixing chamber. The temperature is measured using an AVS-47 resistance bridge and a carbon resistor that has been calibrated against an *in situ* melting curve pressure gauge thermometer.

The heat capacity was obtained by applying dc heat pulses to the calorimeter and measuring the resulting temperature changes. Figure 2 shows the heat capacity of ^{3}He, as a function of the temperature for 0.02 layers $\leqslant N_3 \leqslant 0.93$ layers at a fixed ^{4}He coverage of 3.14 bulk-density atomic layers.[21] The background heat capacity, due to the the sample cell and the ^{4}He coverage, was fit to a polynomial curve and subtracted from all data. As an indication of the size of the background, the background for 3.14 layers of ^{4}He was 0.06154 mJ/K at 60 mK and 0.0798 mJ/K at 100 mK. The effect that changes in N_3 have on the Fermi temperature is seen in Fig. 2.

The lowest-coverage heat capacity data (0.02 ^{3}He layers) is nondegenerate, and the temperature independence of the classical region is observed. At substantially higher coverages, for example, at 0.45 layers, there is data for which $T \ll T_F$ and the linear dependence[22] of C on temperature is observed (Fig. 3). Lines have been drawn through some of the data in the degenerate regime to help guide the eye and emphasize the presence of linearity when $T < T_F$. For the higher ^{3}He coverages, as the temperature increases and the Fermi temperature is approached, the data departs from the linear trend and approaches a constant as expected for the classical regime. Recent heat capacity data for the case of 4.33 layers of ^{4}He, which shows the same general features as the data for 3.14 layers of ^{4}He, is consistent with our earlier work,[14] but extends to lower temperatures.

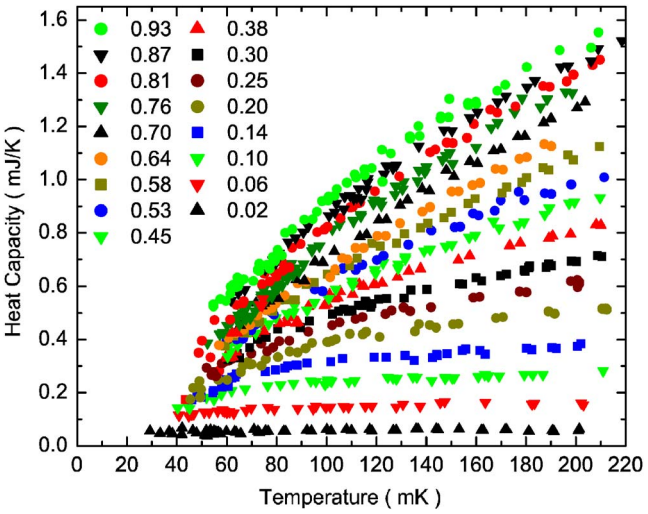

FIG. 2. (Color online) The heat capacity ^{3}He, as a function of the temperature for 0.02 layers $\leqslant N_3 \leqslant 0.93$ layers at a fixed ^{4}He coverage of 3.14 layers.

At selected fixed values of the temperature, one can obtain C/T as a function of ^{3}He coverage from the data. C/T is shown in Fig. 4 for three values of the temperature for the case of 4.33 layers of ^{3}He. Evident in the data is the step in the heat capacity that signals the occupation of the first excited state for the ^{3}He first seen in the magnetization experiments.[11] The effective mass m^* is proportional to C/T [Eq. (3)] and is shown, scaled by the bare ^{3}He mass, on the right axis. A plot of m^*/m versus ^{3}He coverage, where the data is restricted to the degenerate region of the first Fermi disk, is shown in Fig. 5. In the ideal noninteracting case the effective mass of the ^{3}He quasiparticle would be independent of ^{3}He coverage. This is clearly not the case, as has been

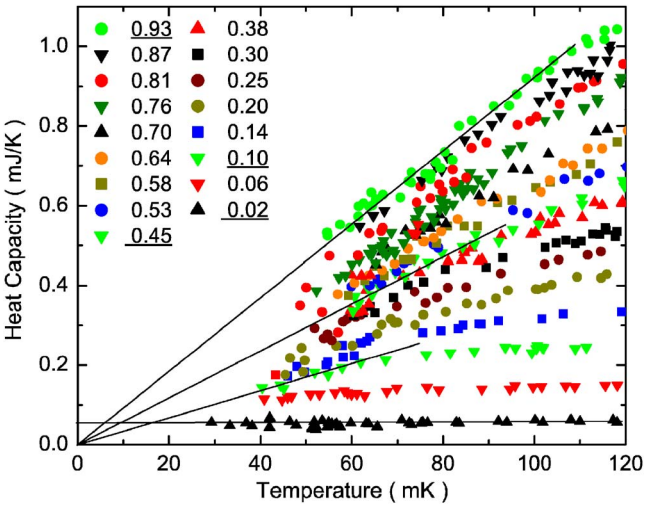

FIG. 3. (Color online) Expanded view of the data shown in Fig. 2. Lines have been added to more clearly show the linear behavior seen in the degenerate and Boltzmann regimes.

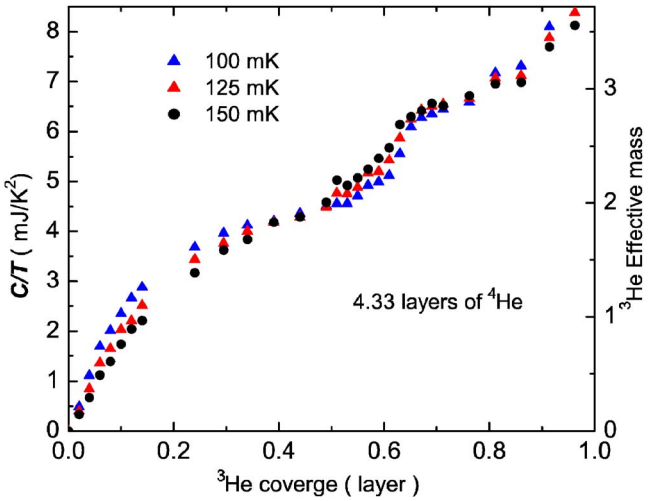

FIG. 4. (Color online) C/T for ^{3}He, as a function of the ^{3}He coverage for 0.02 layers $\leqslant N_3 \leqslant 1$ layers at a fixed ^{4}He coverage of 4.33 layers for three values of the temperature. The effective mass is shown on the right axis.

seen previously. The hydrodynamic mass is found by extrapolating m^* to zero ^{3}He coverage. We find that an increase in the ^{4}He coverage results in a decrease in the hydrodynamics mass. This is expected and is due to the fact that the environment of the free surface is more constrained for a thinner film and the behavior is consistent with theoretical expectations. In particular, Clements *et al.*[23,24] have calculated the hydrodynamic mass for a ^{3}He atom on thin ^{4}He films adsorbed to a graphite substrate. Their calculation assumes that the substrate is covered by two inert layers of solid ^{4}He and, as their standard approach, their coverage values refer to only the liquid portion of the film. The thickness of the solid layer for ^{4}He adsorbed to Nuclepore will be different due to the different strength of the potential provided by the substrate. Sprague *et al.*[25] have determined the

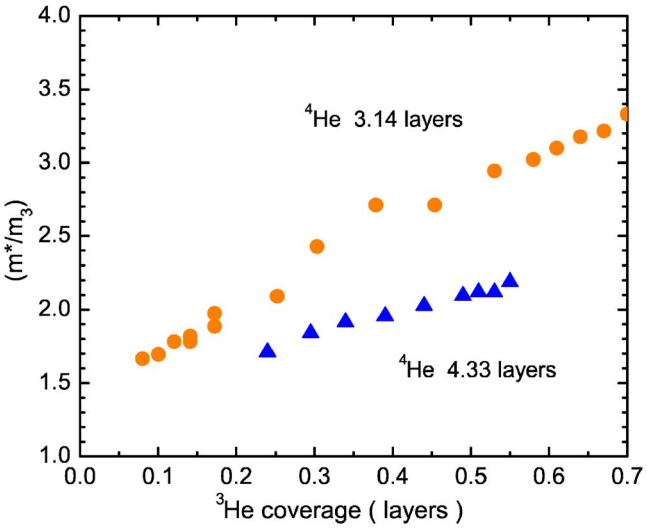

FIG. 5. (Color online) Effective mass vs ^{3}He coverage, where the data is restricted to the degenerate region of the first Fermi disk, is shown for 3.14 and 4.33 layers ^{4}He for $T=100$ mK.

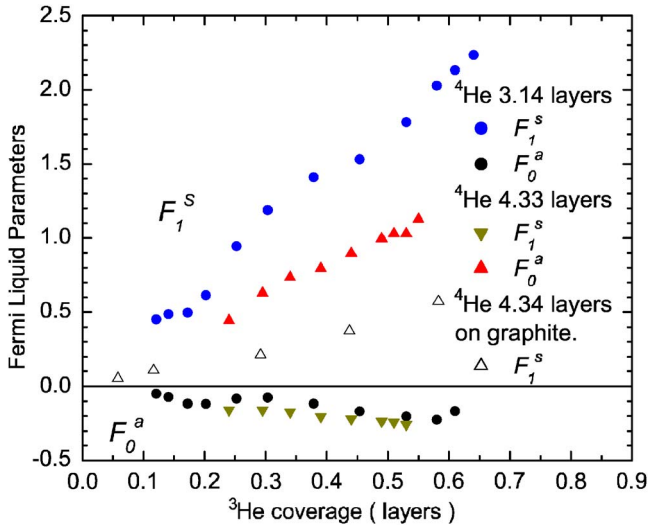

FIG. 6. (Color online) The Fermi liquid parameters F_1^S and F_0^A versus ^{3}He coverage for 3.14 and 4.33 layers ^{4}He. Also shown are the F_1^S values of Dann *et al.* (Ref. 22) obtained for a ^{4}He coverage of 4.34 layers on a graphite substrate.

solid layer thickness of ^{4}He on Nuclepore to be 2.66 bulk-density layers. This value, when combined with the fact that one bulk-density layer is equal to 0.0772 atoms/Å^2, allows us to make a reasonable comparison with the theoretical predictions. Our 3.14 and 4.33 layer coverages should correspond with the Clements *et al.* values of 0.034 and 0.129 atoms/Å^2, respectively. The predicted values for m_H/m_3 are 1.68 for 3.14 layers and 1.36 for 4.33 layers. The experimental values at 100 mK found by linear extrapolation are 1.39 for 4.33 layers and 1.56 for 3.14 layers. Including the m^* data for 60 mK along with that at 100 mK at 3.14 layers yields $m_H/m_3=1.69$.

As mentioned, the Fermi liquid parameter F_1^S represents the p-wave scattering among ^{3}He atoms and is plotted as a function of ^{3}He coverage in Fig. 6. The p-wave scattering is clearly suppressed by increasing the ^{4}He coverage.

The magnetic susceptibility can also be described in terms of the Fermi Liquid parameters. In this case,

$$\frac{\chi}{\chi_0} = \frac{m^*}{m_3}\frac{1}{1+F_0^A}, \tag{5}$$

where χ_0 is the susceptibility of the noninteracting ideal 2D Fermi system and F_0^A represents the s-wave scattering between the ^{3}He quasiparticles. Combining the magnetic susceptibility data of Higley *et al.*[11] with the measurements of m^* (Fig. 5) enables the calculation of F_0^A. The values are shown in Fig. 6. Negative values of F_0^A reflect the enhanced susceptibility caused by interactions. At these temperatures and coverages, the p-wave scattering dominates the s-wave scattering.

In conclusion, we have presented heat capacity measurements for a range of ^{3}He coverages for two values of the ^{4}He coverage, which allows the data to span T_F. We report the measurement of m^* and the Fermi liquid parameter F_1^S. When

combined with previous magnetic susceptibility data, these data allow the calculation of F_0^A as a function of ^{3}He coverage at two different coverages of ^{4}He. Increasing the ^{4}He coverage, decreases the hydrodynamic mass and suppresses the *p*-wave scattering among the ^{3}He quasiparticles. *p*-wave scattering dominates the interaction over *s*-wave scattering.

This work was supported by the National Science Foundation through Grant Nos. DMR 0138009 and by Research Trust Funds administered by the University.

*Nano-Science Laboratory, RIKEN, Hirosawa, Wako-City, Saitama 351-0198, Japan.

[1] G. K. Walters and W. M. Fairbank, Phys. Rev. **103**, 262 (1956).
[2] A. F. Andreev, Sov. Phys. JETP **23**, 939 (1966).
[3] D. O. Edwards and W. F. Saam, in *Progress in Low-Temperature Physics*, edited by D. F. Brewer (North-Holland, Amsterdam, 1978), Vol. 7A, Chap. 4, p. 284.
[4] R. B. Hallock, Phys. Today **51** (6), 30 (1998).
[5] R. B. Hallock, Physica B **329–333**, 154 (2003).
[6] R. B. Hallock, in *Progress in Low-Temperature Physics*, edited by W. B. Halperin (North-Holland, Amsterdam, 1995), Vol. 14, Chap. 5, p. 321.
[7] There is some debate as to whether the width of the ^{4}He free surface is adequate to hold two states or just one; see, for example, N. Pavloff and J. Treiner, J. Low Temp. Phys. **83**, 15 (1991). For our relatively low ^{3}He coverages, this will not be important.
[8] F. M. Gasparini, B. Bhattacharyya, and M. J. DiPirro, Phys. Rev. B **29**, 4921 (1984); D. S. Sherrill and D. O. Edwards, *ibid.* **31**, 1338 (1985).
[9] E. Krotscheck, Phys. Rev. B **32**, 5713 (1985); B. E. Clements, E. Krotscheck, and M. Saarela, *ibid.* **55**, 5959 (1997).
[10] B. Bhattacharyya and F. M. Gasparini, Phys. Rev. Lett. **49**, 919 (1982).
[11] R. H. Higley, D. T. Sprague, and R. B. Hallock, Phys. Rev. Lett. **63**, 2570 (1989).
[12] B. Baym and C. Pethick, in *The Physics of Liquid and Solid Helium, Part II*, edited by K. H. Bennemann and J. B. Ketterson (Wiley, New York, 1978), Vol. 29, Chap. 1, p. 1.
[13] P.-C. Ho and R. B. Hallock, J. Low Temp. Phys. **121**, 501 (2000).
[14] P.-C. Ho and R. B. Hallock, Phys. Rev. Lett. **87**, 135301 (2001).
[15] P.-C. Ho, H. Akimoto, and R. B. Hallock, J. Low Temp. Phys. **126**, 349 (2002).
[16] H. Akimoto and R. B. Hallock, Physica B **329–333**, 164 (2003).
[17] H. Akimoto and R. B. Hallock, J. Low Temp. Phys. **134**, 257 (2004).
[18] Corning Inc., Separation Div., 45 Nagog Park, Acton, MA, 01720.
[19] M. J. DiPirro and F. M. Gasparini, Phys. Rev. Lett. **44**, 269 (1980); J. M. Valles, Jr., D. T. Smith, and R. B. Hallock, *ibid.* **54**, 1528 (1985).
[20] P.-C. Ho and R. B. Hallock, J. Low Temp. Phys. **121**, 797 (2000).
[21] Here, 3.14 bulk-density atomic layers means that the film would have a thickness of 3.14×0.36 nm$=1.13$ nm if the entire film were at the density of bulk helium. The atoms adjacent to the substrate are at higher density. Thus, the actual thickness of the film is less than 1.13 nm in this case. Based on our earlier measurements with third sound in the NMR apparatus, 3.14 bulk-density atomic layers is equivalent to an actual film thickness (distance from the substrate surface to the free surface of the ^{4}He film) of $(3.14-1.33) \times 0.36$ nm$=0.65$ nm; 4.33 bulk-density layers corresponds to an actual film thickness of 1.08 nm, of which we expect 0.36 nm is fluid.
[22] Degenerate heat capacity results have also been obtained for mixture films on graphite [M. Dann, J. Nyeki, B. P. Cowan, and J. Saunders, Phys. Rev. Lett. **82**, 4030 (1999)].
[23] E. Krotscheck, M. Saarela, and J. L. Epstein, Phys. Rev. Lett. **61**, 1728 (1988); J. L. Epstein, E. Krotscheck and M. Saarela, *ibid.* **64**, 427 (1990); B. E. Clements, E. Krotscheck, and M. Saarela, *ibid.* **55**, 5959 (1997).
[24] B. E. Clements, E. Krotscheck, and M. Saarela, J. Low Temp. Phys. **100**, 175 (1995).
[25] D. T. Sprague, N. Alikacem, and R. B. Hallock, Phys. Rev. Lett. **74**, 4479 (1995).